Appendix

Upcycling waste protein and heavy metal into single-atom catalytic gas diffusion electrode for CO_2 reduction

Baiqin Zhou, Zhida Li, Chunyue Zhang, Lu Lu*

State Key Laboratory of Urban Water Resource and Environment, School of Civil and Environmental Engineering, Harbin Institute of Technology, Shenzhen, Shenzhen 518055, China

*Corresponding author E-mail: lulu@hit.edu.cn

Experimental procedures

Synthesis of electrode for oxygen evolution

In the MEA, the counter electrode was a 4 cm^2 titanium mesh (100 mesh) with IrO_2 coating. Briefly, a titanium mesh was heated in 6 M HCl at 85℃ to sweep surface impurity. Then the mesh was drop-cast by $H_2IrCl_6 \cdot xH_2O$ solution (1 mL solution consisted 10mg $H_2IrCl_6 \cdot xH_2O$, 900 μL isopropanol and 100 μL 6 M HCl), and followed with heating at 100℃ for 10 min. The dried mesh was further calcinated at 500℃ for 10 min to form IrO_2 coating. This process was triplicated to achieve a suitable 2 mg/cm^2 $H_2IrCl_6 \cdot xH_2O$ loading.

Evaluation of turnover frequency (TOF)

TOFs/h for ECO_2RR products were evaluated based on 2 calculation methods. The first is the electrochemical active surface area (ECSA) normalization. Proposed by Jiang *et al*. [1] and Chen *et al*. [2], the ECSA of SP_{GDE} and NP_{GDE} were calculated to 404.6 cm^2 and 357.90 cm^2 according to 21 μF/cm^2 of reported electrochemical double layer capacity (EDLC) of graphene (Fig. S17, Ref. 1 and 2). Then the moles of C atoms were estimated by the formula: ESCA/(specific surface area)×12 (11.97 m^2/g for SP_{GDE} and 16.39 m^2/g for NP_{GDE}). And considering the Ni atomic content in the membrane electrode (XPS result, Fig. S7 and S8), accordingly number of Ni sites in SP_{GDE} and NP_{GDE} were 1.06×10^{-8} and 1.02×10^{-8}, respectively. Then TOFs based on ESCA normalization was calculated by $(j_{total}\times t\times FE_{CO})/(2F\times$the number of Ni sites).

Mass loading normalization TOFs were calculated by mass loading of Ni in the catalyst. The number of Ni sites were calculated by (catalyst loading mass × Ni mass content)/58, Ni mass contents were 3.75 wt% and 2.41 wt% for SP_{GDE} and NP_{GDE}, respectively. Accordingly, TOFs were calculated as the formula aforementioned.

Calculation of potential extraction amounts of protein from agriculture & food waste

According to the Food and Agriculture Organization of the United Nations (FAO) statics, 7 kinds of agriculture & food waste amount were reported in the latest *Global Food Losses and Wastes* [3].

The calculation in our study referred statics provided by FAO. But due to the inexact data provided, we provided some approximate data according to the statics charts in FAO's report [3]. We also gave the protein content and annual yield of several agriculture & food representative in each category; the comprehensive protein content of each category was calculated from weighted average of main subdivision of each category (Table S2 to S3) since no exact wasted agriculture & food amount was provided by FAO [3]. Total wasted agriculture & food amounts were calculated via comprehensive lost & wasted rate of 7 macro regions multiply approximate data of 7 kinds of agriculture & food production. All data were summarized in Table S2 to S3.

Lost & wasted amount was calculated as bellow:

Lost & wasted amount $=\sum_{i=1}^{7}$ Each category production of each macro region × comprehensive lost & wasted rate

Where, *i* represents 7 macro regions mentioned in Table S3.

Potential extracted protein amount was calculated based on the following:

Potential protein extraction amount = production × comprehensive protein content

Comprehensive protein content = $\sum_{i=1}^{n} x_i \times$ average protein content

Where, x_i represents the main subdivision production in each category.

Calculation of potential CO_2 capture when using SP_{GDE} in practice under renewable electricity driving

Considering the durability of each SP_{GDE} was 8 h, and average 90% FE_{CO} (Fig. 5f) during operation under 50 mA/cm^2, the annual CO_2 capture amount per ton of extracted protein was as follows:

CO_2 capture amount = $x_{CO} \times v \times 60 \times 24 \times 365$ / [extracted protein amounts in per cm^2 × (365 × 24 / 8)]

Where, x_{CO} represents the volume fraction of CO; v is the flow rate; extracted protein amount in per cm^2 was calculated as below:

Extracted protein amount in per cm^2 = protein addition during electrospinning × pristine SP_{GDE} area × contraction factor

Where, the pristine SP_{GDE} was around 450 cm^2 with 10 g extracted protein as the feedstock. After preoxidation and carbonization, the final SP_{GDE} shrank to around 0.7 area of the pristine one, thus the contraction factor was 0.7.

Energy input to synthesize SP_{GDE}

In this study, we only consider the extracted protein listed in Table S3 and S4. According to the energy limitation to produce common graphene (6440 kW·h/t), converting all extracted protein into SP_{GDE} needs 125.5 million tons × 6440 kW·h/t = 808.22 billion kW·h, which equals to 99.33 million tons standard coal combustion (1 kW·h electricity generation needs 0.1229 kg standard coal combustion). The total C combustion reaches to 66.18 million tons and correspond 123.51 billion m^3 CO_2 emission (1 ton standard coal contains 0.67 tons C, this data was suggested by Nation Development and Reform Commission of China. And 1 ton C combustion equals 3.67 tons or 1866.33 m^3 CO_2 emission).

Implications toward carbon reduction and heavy metal recovery

The annual generation of vast wastes worldwide has underscored the need for mitigating both environmental pollutants and CO_2 emissions effectively. In this context, we introduce ECO_2RR by SP_{GDE} as a promising approach to reuse organic wastes for carbon mitigation. Due to the incredible magnitude of production annually, we investigate the potential of agriculture & food wastes as the protein-enriched resources to synthesize SP_{GDE}. A 2011 report by the Food and Agriculture Organization of the United Nations (FAO) notes that around 1.3 billion tons global agriculture & food wastes are produced annually, including 7 categories — cereals, roots and tuber, oilcrops and pulses, fruits and vegetables, meat, fish and diary (Gustavsson et al., 2011). Based on the protein content of these 7 categories (summarized in Table S2 and S3), available waste protein amounts are expected to be ~251 million tons, corresponding to ~125 million tons C (considering 50 wt% C content in protein) that can be sequestrated by carbonization of waste protein to produce the electrode material. The corresponding energy required to produce SP_{GDE} is estimated to 808 billion kW·h annually, which equals to 99 million tons standard coal combustion. Totally, if the strategy of this study is used, more than 353 million tons C can be converted into several

chemicals and more than 125 million tons C are fixed into SP_{GDE} itself. Moreover, 5 million tons heavy metals can be recovered for SACs synthesis.

Table S1 XPS result of Ni content (atom ratio) in GDEs

NP_{GDE}	SP_{GDE}
0.26%	0.39%

Table S2 The main subdivisions of agriculture & food

Cereals [3, 4]			
Rice	Maize	Wheat	
498.8-509.9 (7%)	1119.7-1208 (3.8%)	762.2-778.6 (8%-16%)	
Roots and tubers [4, 5]			
Potato	Sweet potato		
~376 (1.6%-2.1%)	~145 (1.6%-2.1%)		
Oilcrops and pulses [4, 6]			
Soybean	Peanut	Rape	
~380 (35%-50%)	~44 (24%-36%)	~68 (21.96%-26.15%)	
Vegetables and fruits [7]			
Vegetable	Fruit		
~1380 (<1%)	~883 (<1%)		
Meats [4, 8]			
Pork	Beef	Chicken	Mutton
96-111 (13.2%)	~58 (26.33%)	928-991 (20%)	~15 (20%)
Fish [9]			
~179 (18%)			
Diary [4]			
10161-11555 (2.8%-3.8%)			

Note: 1. Unit: million tons; 2. Statistics in brackets are protein content;

Table S3 Wasted agriculture & food amount and rate in 7 macro regions, and potential protein extraction amount

Lost & wasted rate						
Europe	North America, Oceania	Industrialize Asia	Sub-Sahara Africa	North Africa, West and Central Asia	South and Southeast Asia	Latin America
~52%	~60%	~48%	~45%	~33%	~41%	~40%
Lost & wasted amount						
Cereals	Roots and tubers	Oilcrops and pulses	Fruit and vegetables	Meat	Fish	Diary
~1114 (6.99%)	~372 (1.85%)	~255 (38.83%)	~749 (1%)	~120 (19.54%)	~76 (18%)	~350 (3.3%)
Potential protein extraction amount						
Cereals	Roots and tubers	Oilcrops and pulses	Fruit and vegetables	Meat	Fish	Diary
~78	~7	~99	~7	~23	~14	~12

Note: 1. Unit: million tons; 2. Statistics in brackets are comprehensive protein content.

Table S4 Compositions of SP processing wastewater (mg/L)

COD_{Cr}	BOD_5	pH	Total soluble protein
15000 ± 125	8500 ± 80	5.0 ± 0.1	10000 ± 100
Na	K	Ca	Mg
271 ± 22	455 ± 161	74 ± 19	81 ± 33
Fe	S		
17 ± 5	368 ± 82		

Table S5 Compositions of electroplating wastewater (mg/L)

Ni	Al	Cd	Co	Cu	Fe	Mn	Pd	Zn
182.94	9.40	1.58	0.20	1.26	12.59	0.12	0.29	4.48

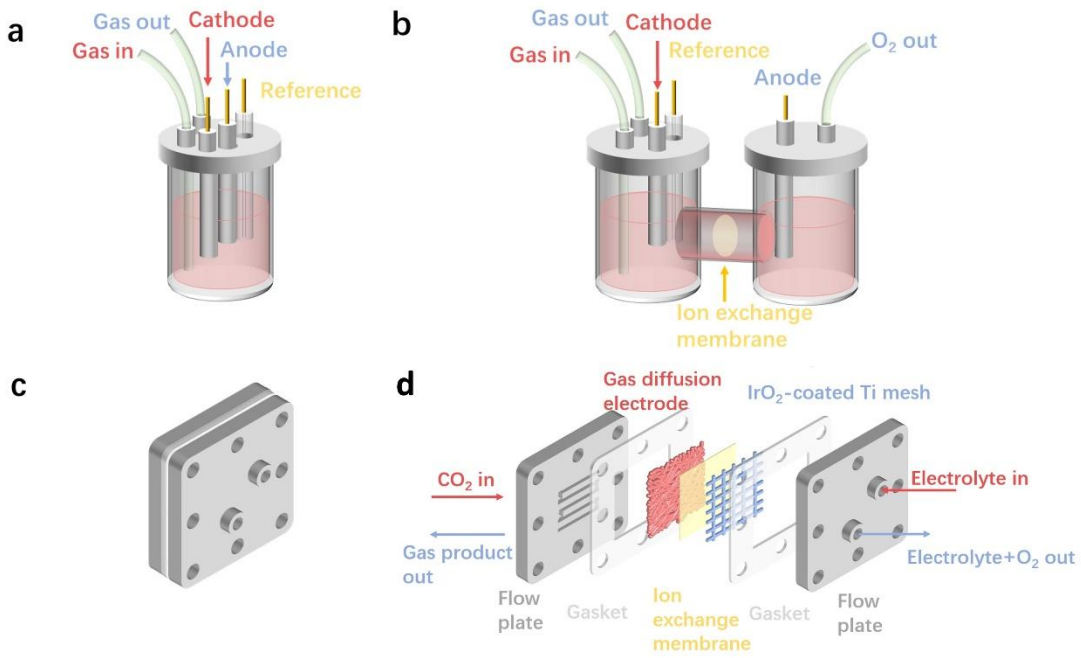

Fig. S1 Electrochemical CO_2RR electrolysis cell. **(a)** Traditional single chamber cell. **(b)** Traditional H-type cell. **(c)** and **(d)** Membrane electrode assembly.

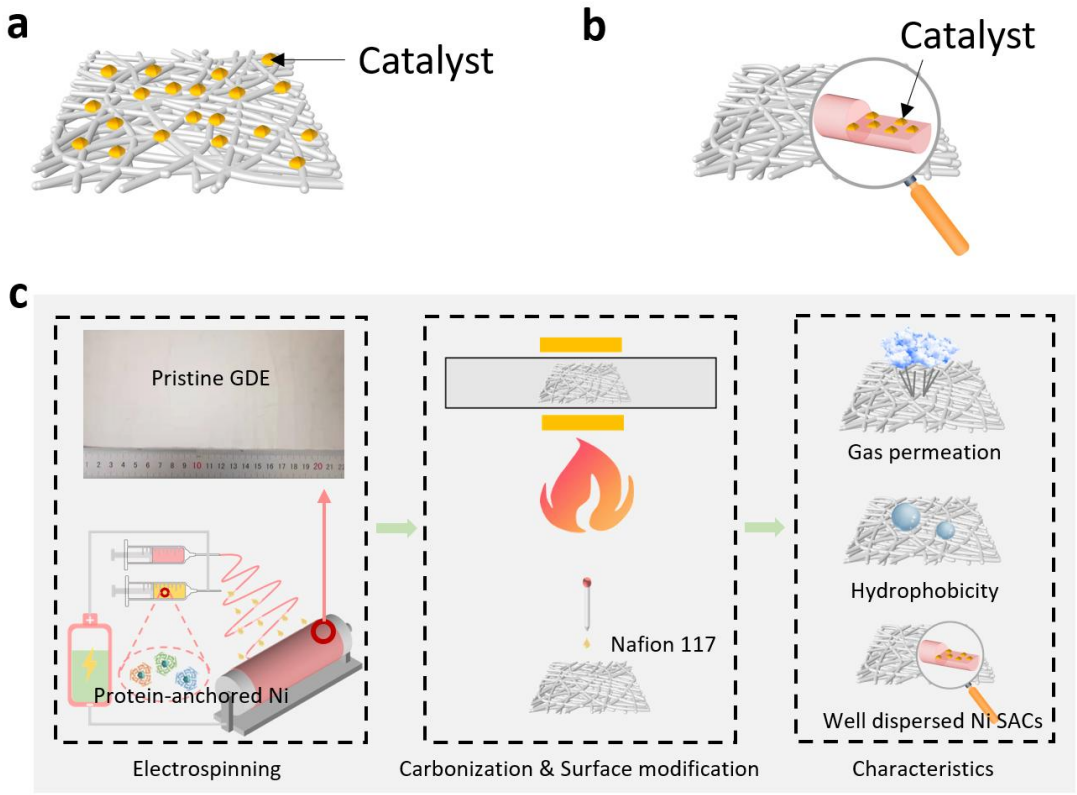

Fig. S2 Gas diffusion electrode (GDE). **(a)** Traditional GDE with catalysts slathering onto a gas diffusion layer (GDL). **(b)** An integrated gas diffusion electrode with Ni SACs inserting into the nanofibers of GDL, proposed by Yang *et al*. [10] **(c)** An overview of protein as the carbon matrix for GDE synthesis and its characteristics.

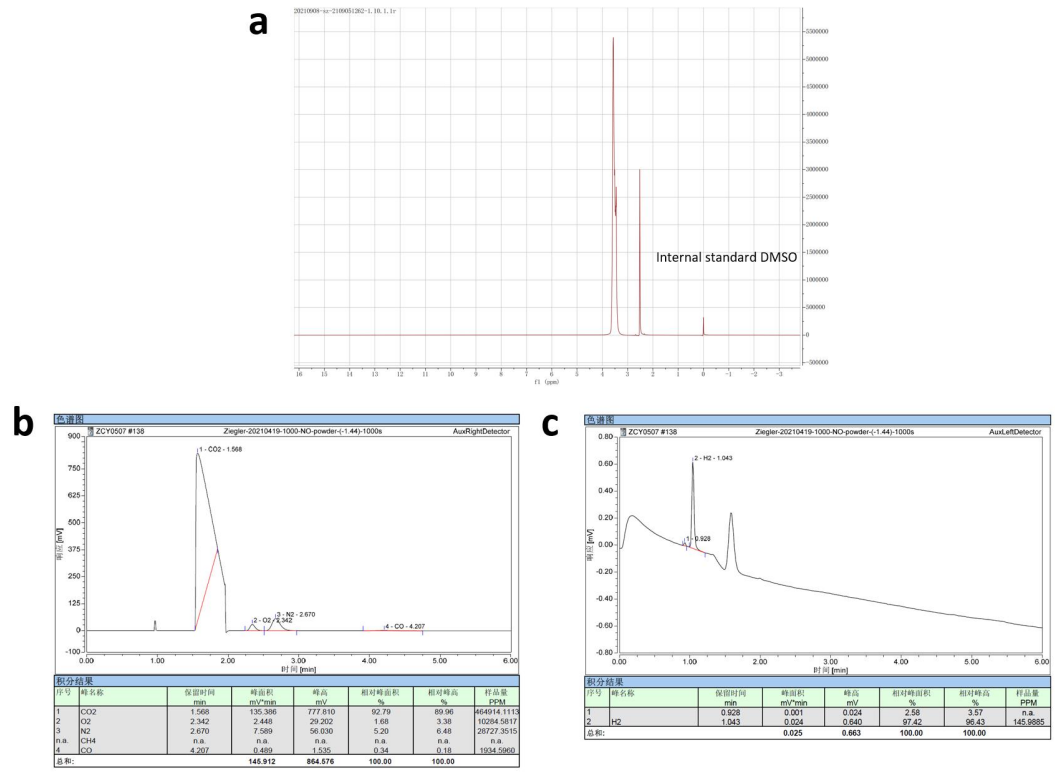

Fig. S3 ECO_2RR products analysis. **(a)** ^1H NMR spectra of 0.5M $KHCO_3$ undergoing 10 h ECO_2RR with powdered SP_{GDE} as the working electrode under -0.8 V vs RHE. **(b)** and **(c)** Gas chromatography analysis of the main gas products under -0.8 V vs RHE.

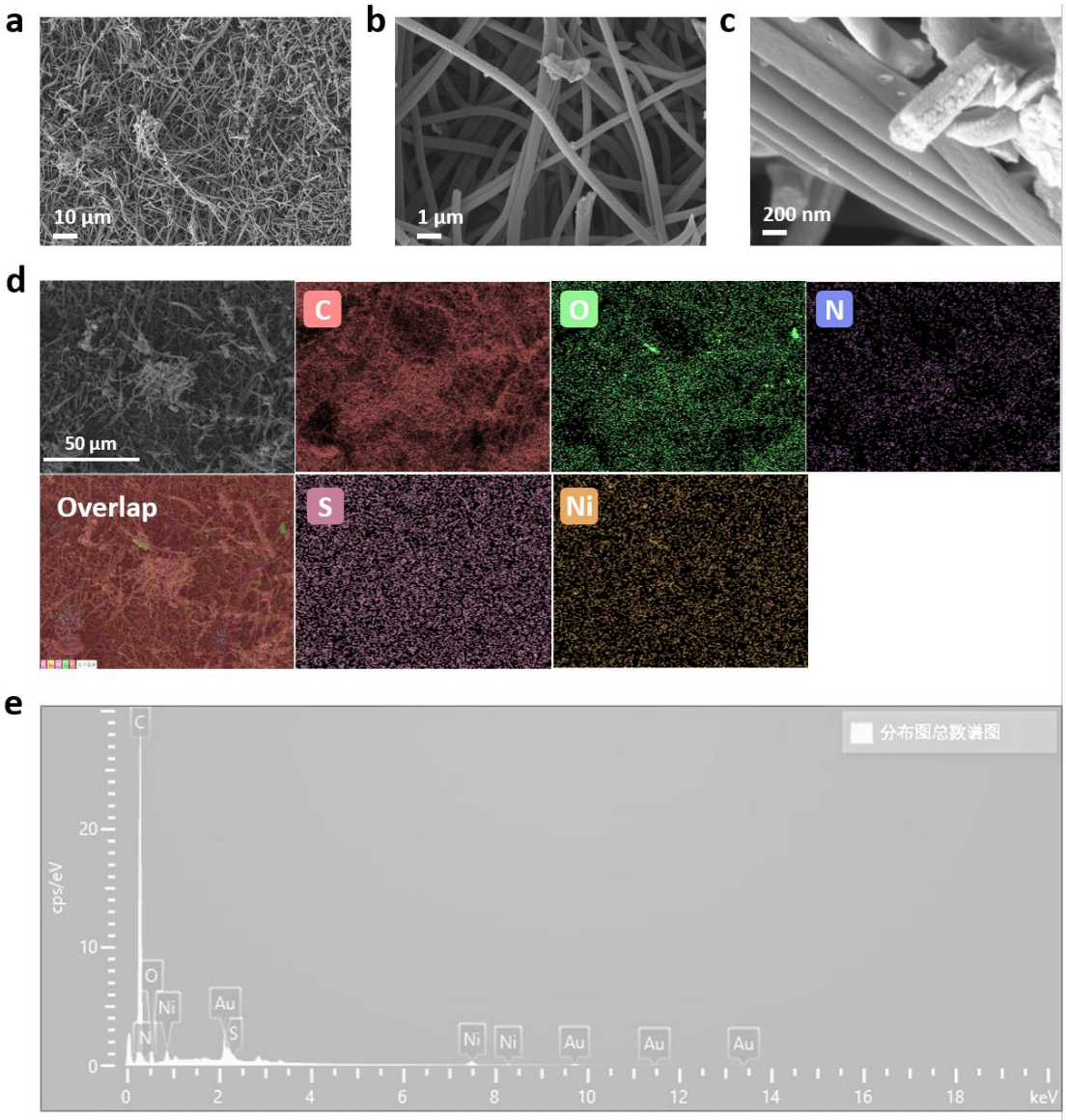

Fig. S4 Surface texture of SP_{GDE} and elemental distribution. **(a)** to **(c)** SEM image. **(d)** Elemental mapping. **(e)** EDS spectra.

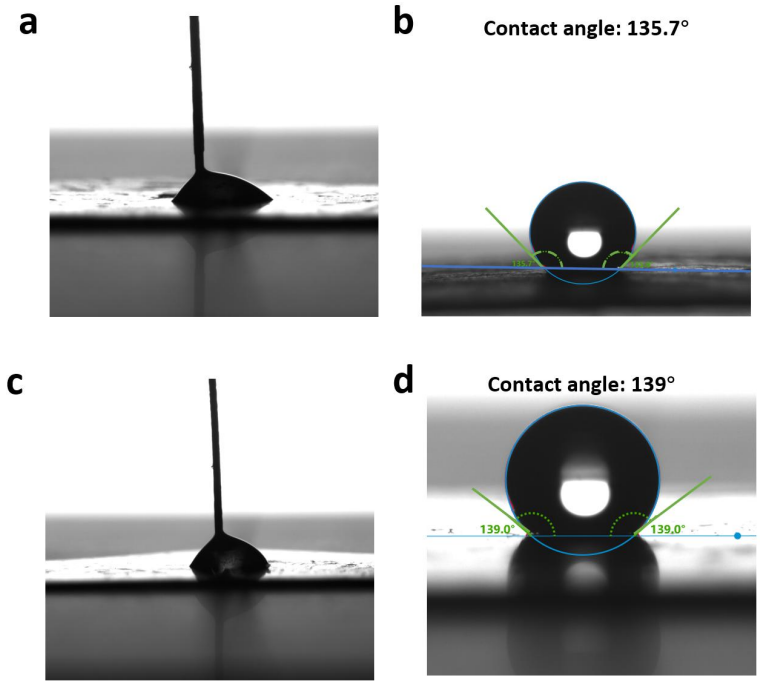

Fig. S5 Contact angle measurement of SP_{GDE} surface and NP_{GDE} surface. **(a)** Hydrophilic nature of SP_{GDE} surface. **(b)** Hydrophobic nature of SP_{GDE} surface with 5 wt% Nafion 117 solution modification, the contact angle is 135.7°. **(c)** Hydrophilic nature of NP_{GDE} surface. **(d)** Hydrophobic nature of NP_{GDE} surface with 5 wt% Nafion 117 solution modification, the contact angle is 139°.

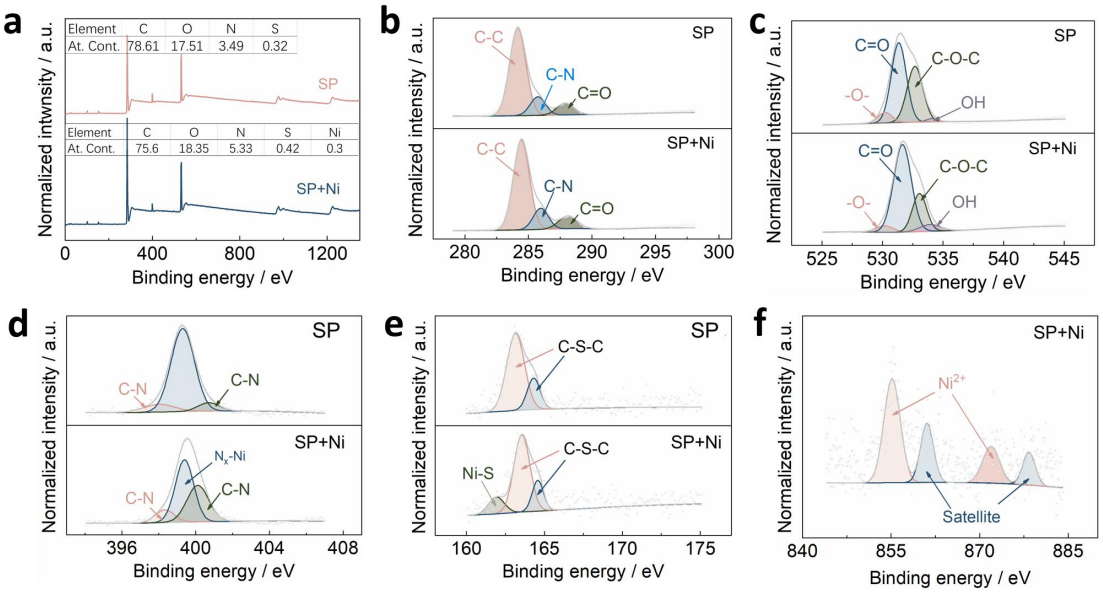

Fig. S6 XPS spectra of reclaimed SP and SP anchoring Ni (SP+Ni). **(a)** Full spectrum. **(b)** C 1s. **(c)** O 1s. **(d)** N 1s. **(e)** S 2p. **(f)** Ni 2p.

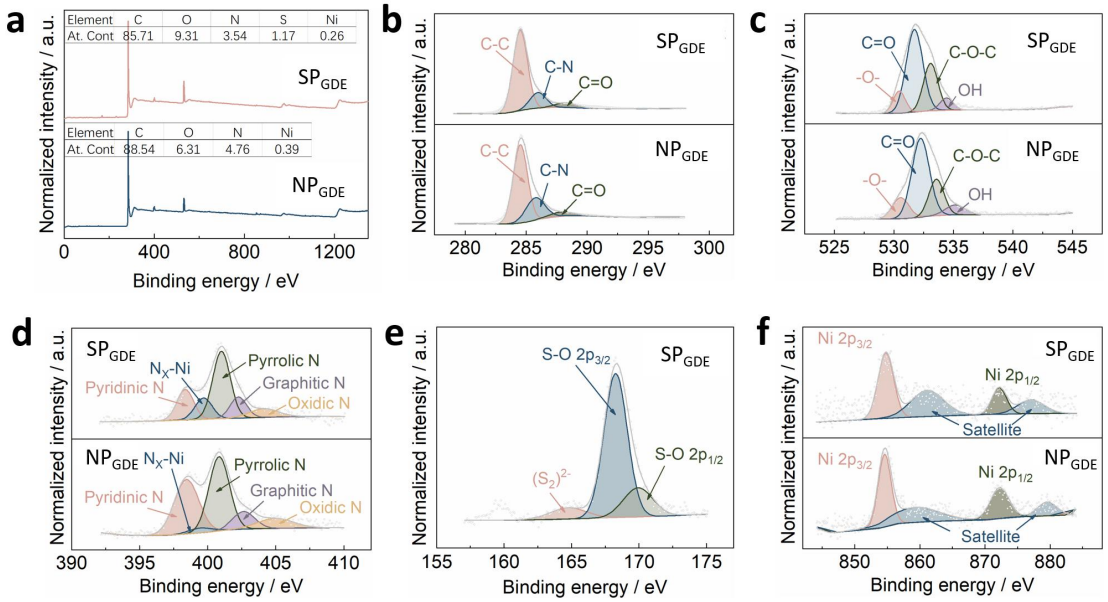

Fig. S7 XPS spectra of SP_{GDE} and NP_{GDE}. **(a)** Full spectrum. **(b)** C 1s. **(c)** O 1s. **(d)** N 1s. **(e)** S 2p. **(f)** Ni 2p.

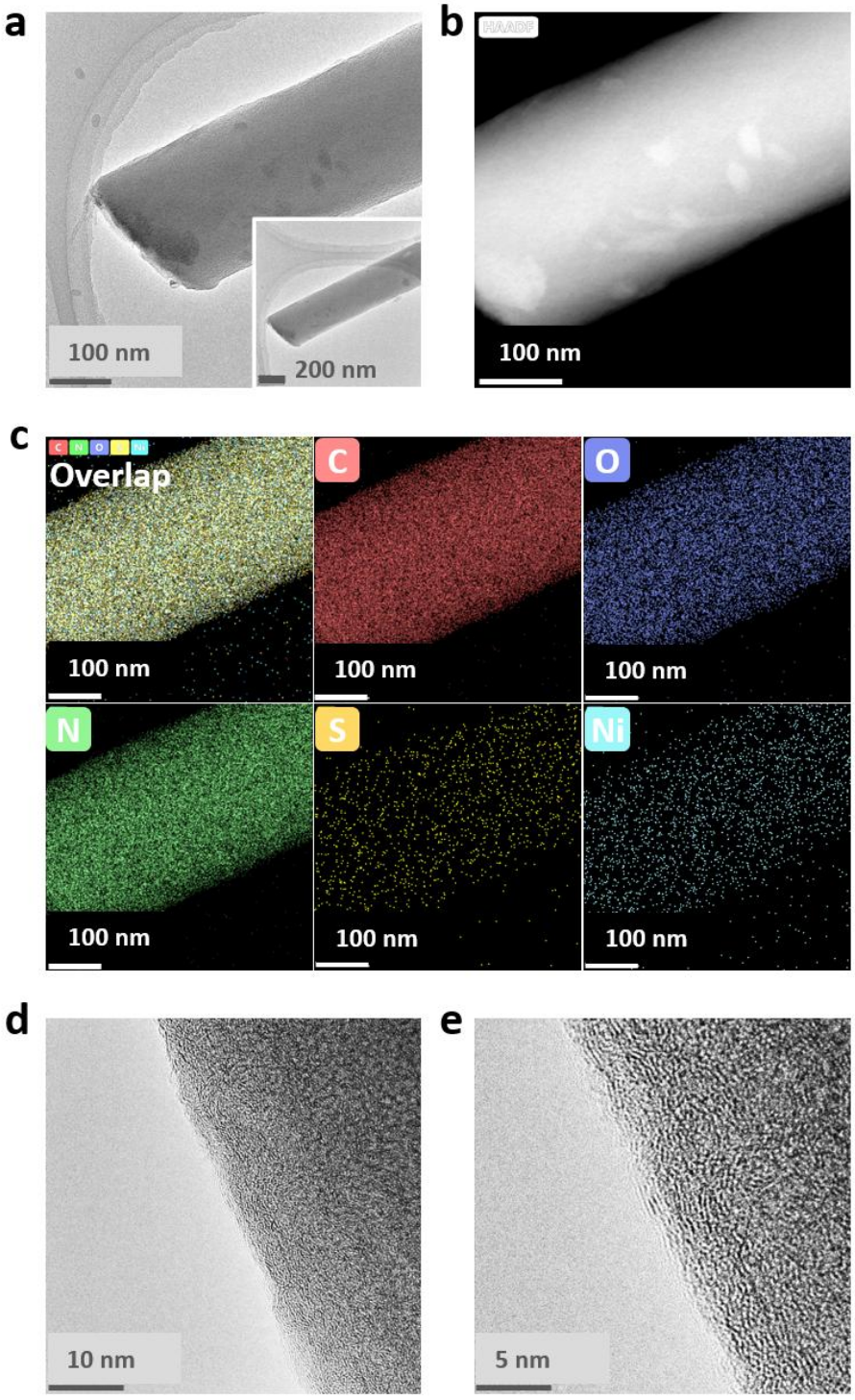

Fig. S8 TEM images of SP_{GDE}. **(a)** to **(c)** TEM, HAADF-TEM and corresponding elemental mapping of a SP_{GDE} nanofiber. **(d)** and **(e)** TEM images of nanofiber's carbon matrix.

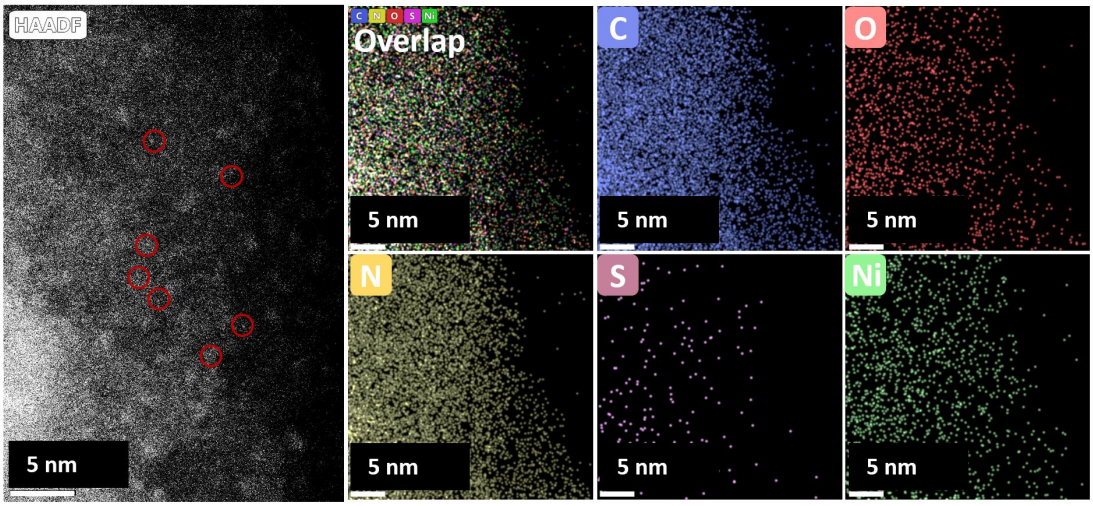

Fig. S9 AC-HAADF-STEM image and corresponding elemental mapping of SP_{GDE}.

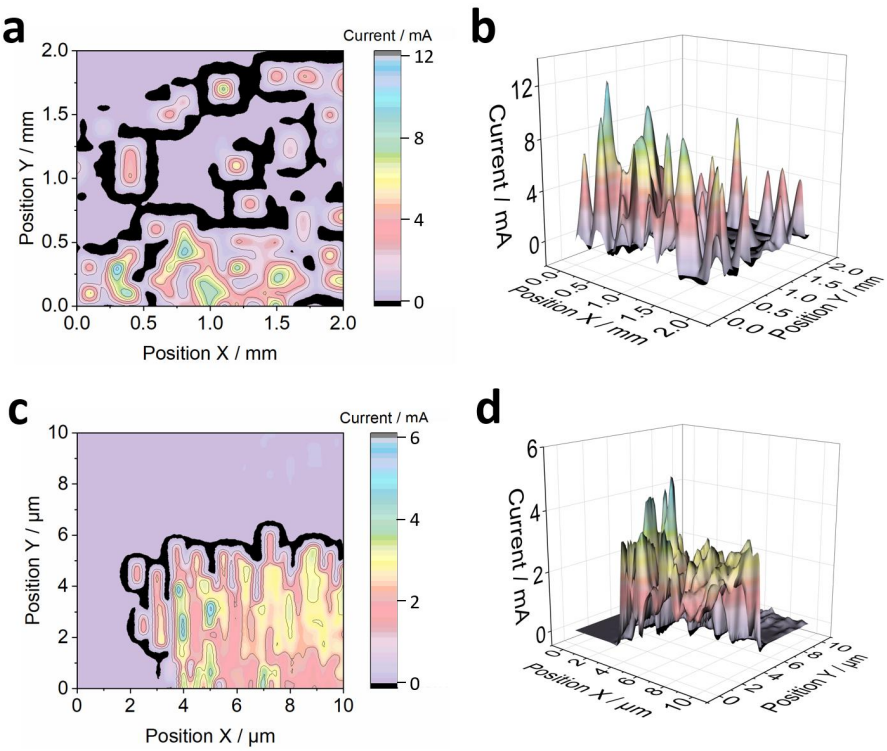

Fig. S10 Scanning Electrochemical Microscopy images of boarder between SP_{GDE} and epoxy resin. Size: 2 mm×2 mm (**a** and **b**), 10 μm×10 μm (**c** and **d**). Step length: 100 μm (**a** and **b**), 250 nm (**c** and **d**).

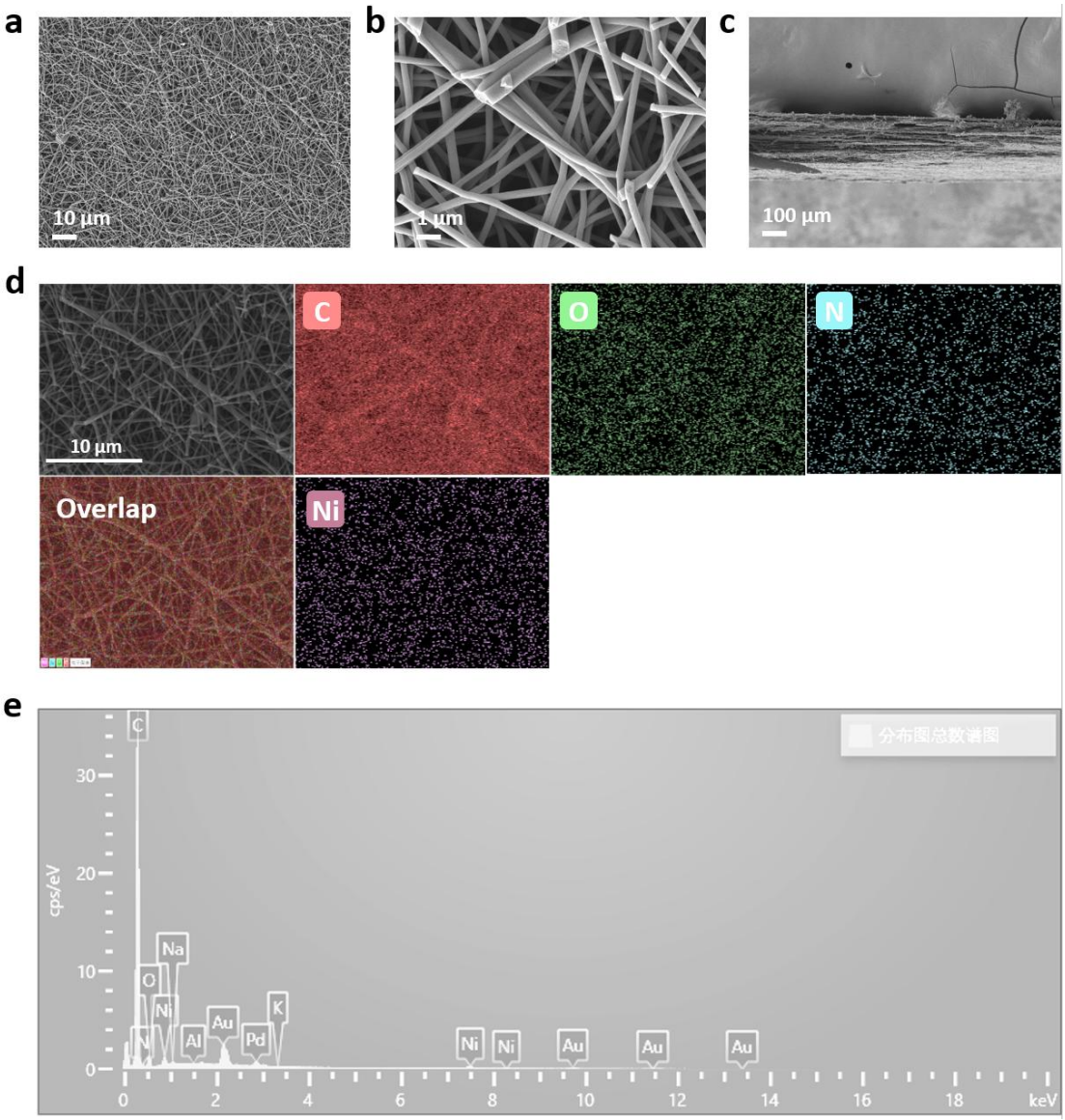

Fig. S11 Surface texture of NP_{GDE} and element distribution. **(a)** and **(b)** Surface SEM image. **(c)** Sectional SEM image. **(d)** Elemental mapping. **(e)** EDS spectra.

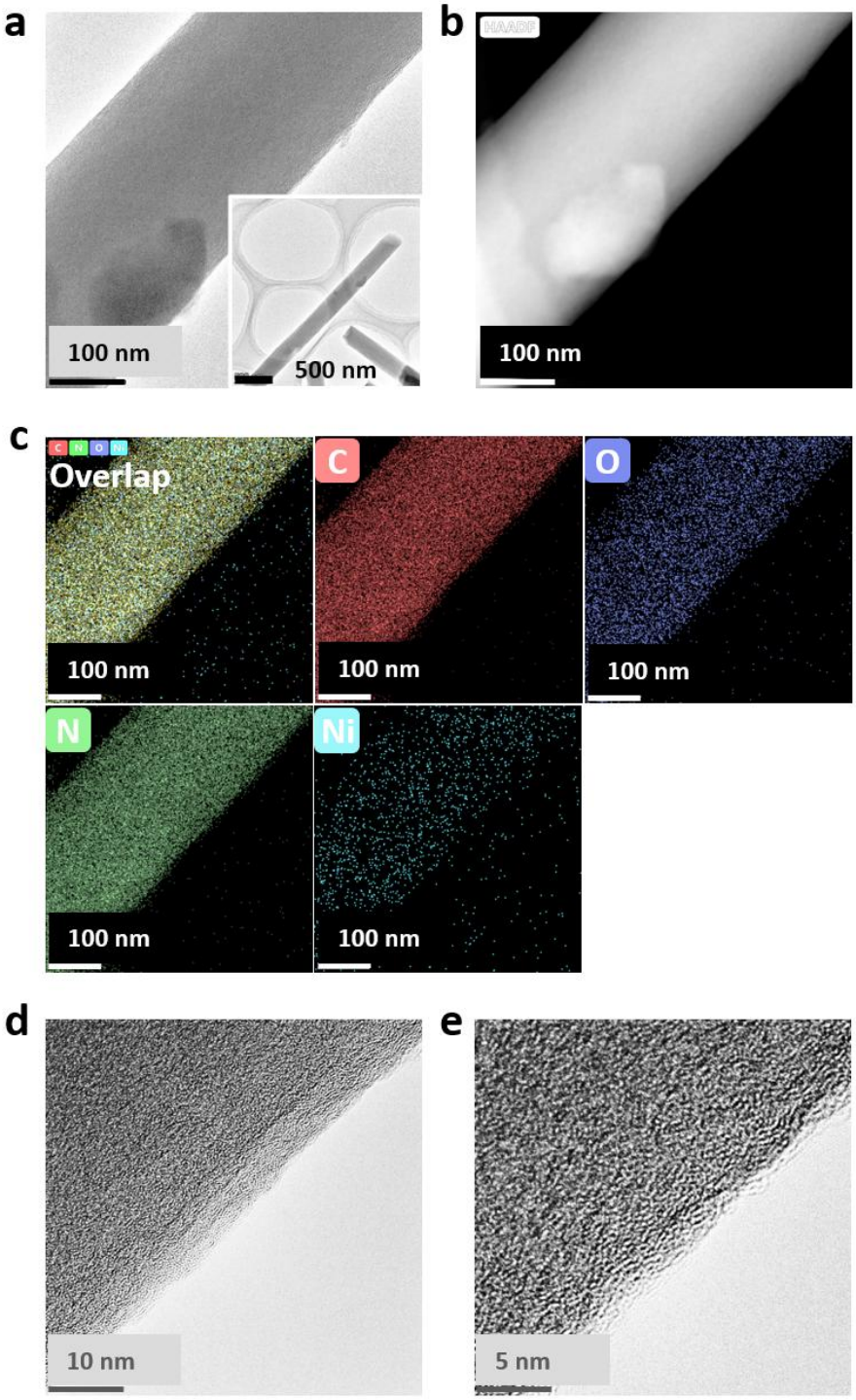

Fig. S12 TEM images of NP_{GDE}. **(a)** to **(c)** TEM, HAADF-TEM and corresponding elemental mapping of NP_{GDE} nanofiber. **(d)** and **(e)** TEM images of nanofiber's carbon matrix.

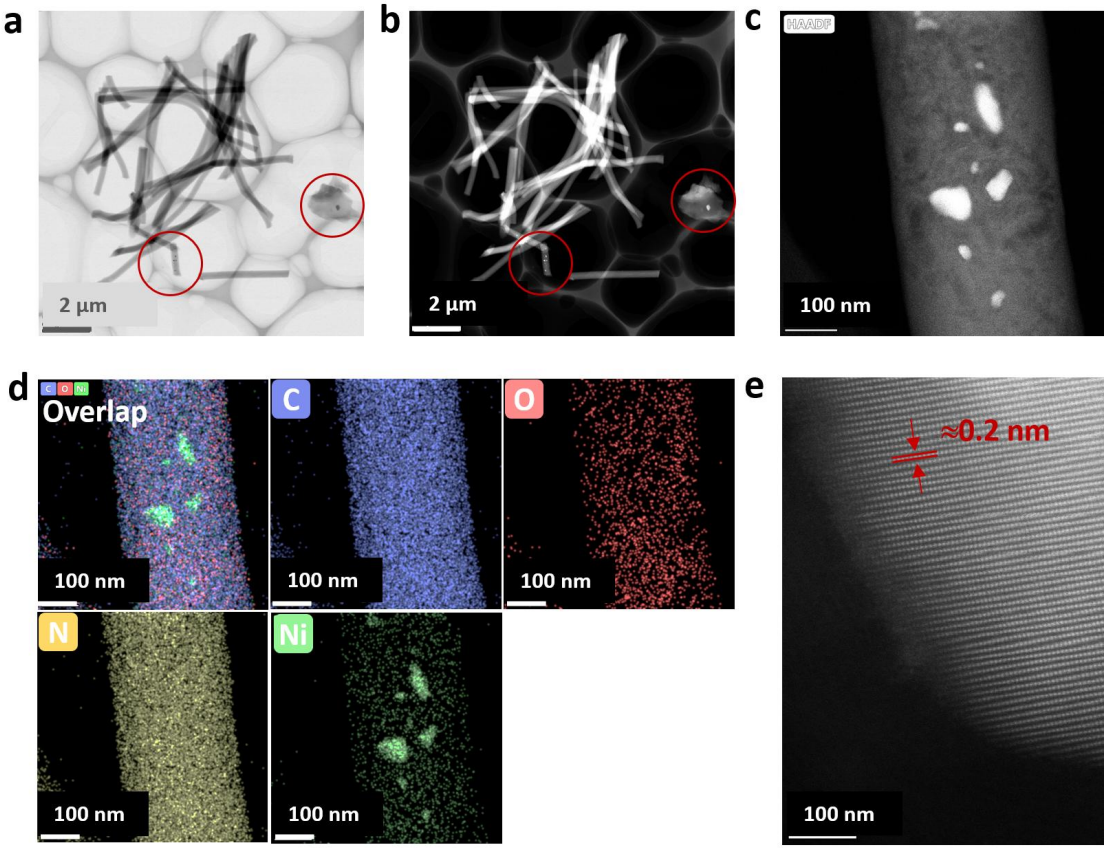

Fig. S13 AC-HAADF-STEM images of NP_{GDE} nanofibers. **(a)** STEM of nanofibers of NP_{GDE}. **(b)** to **(d)** HAADF-STEM of nanofibers of and corresponding elemental mapping. **(e)** Fringe pattern of Ni (111) originated from Ni nanoparticles onto the surface of NP_{GDE} surface.

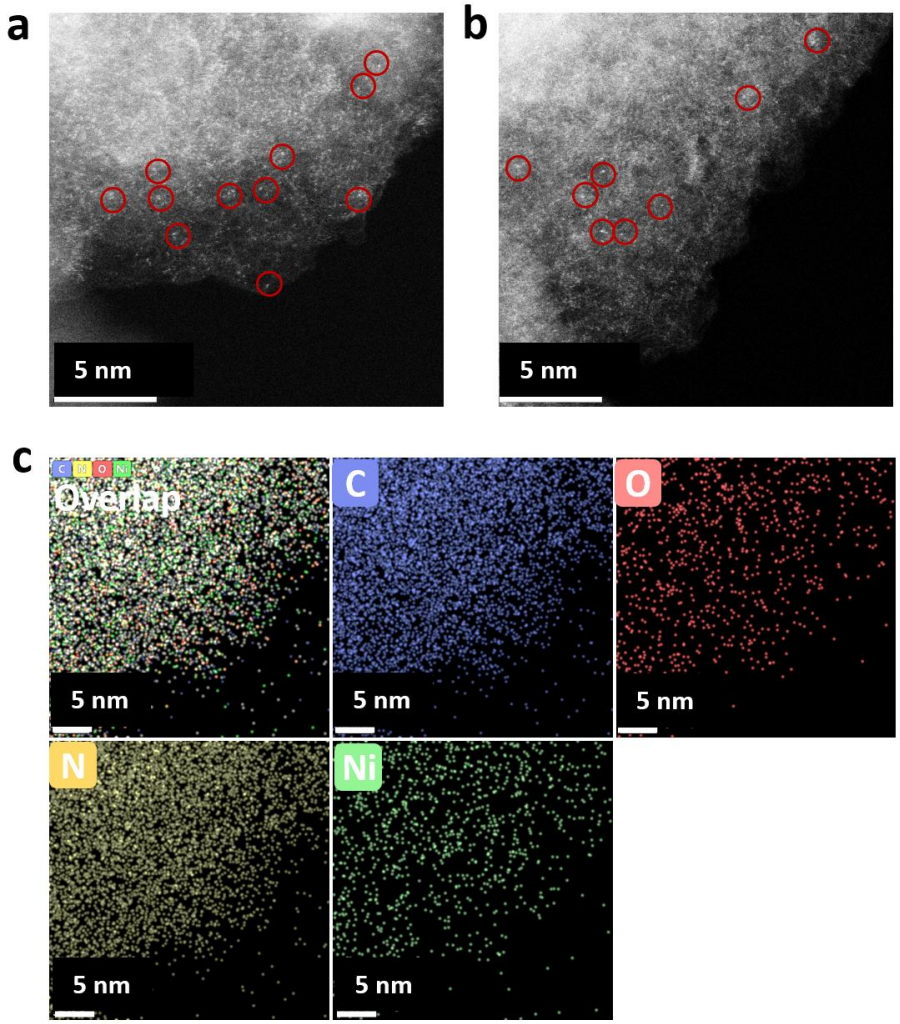

Fig. S14 AC-HAADF-STEM image on different sites and corresponding elemental mapping of NP_{GDE}.

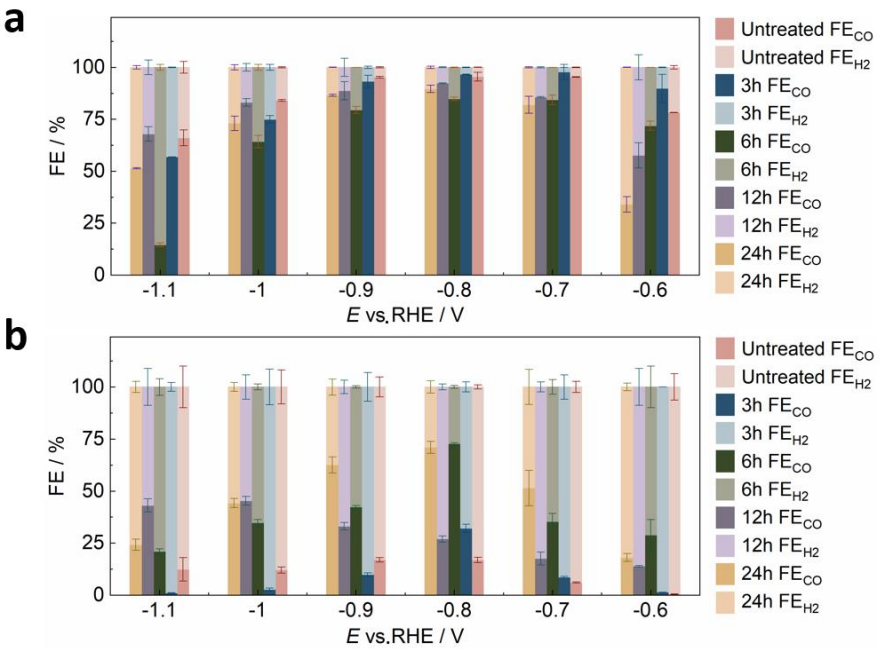

Fig. S15 ECO_2RR performance of SP_{GDE} and NP_{GDE} when treated with different acid (2 M H_2SO_4) soaking time. **(a)** SP_{GDE}. **(b)** NP_{GDE}.

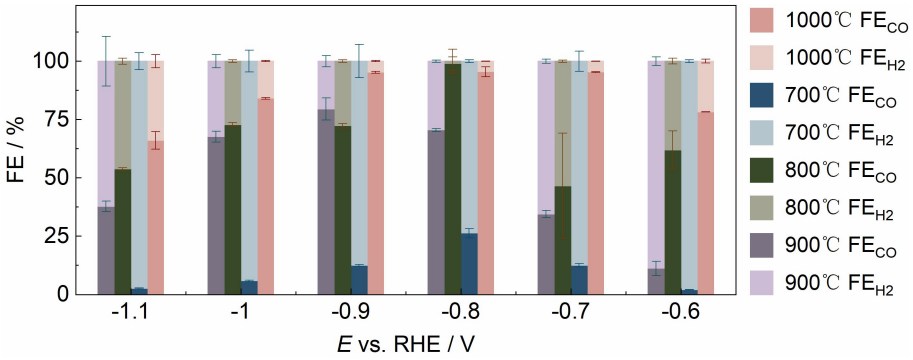

Fig. S16 ECO_2RR performance of SP_{GDE} carbonized at 700℃, 800℃, 900℃ and 1000℃.

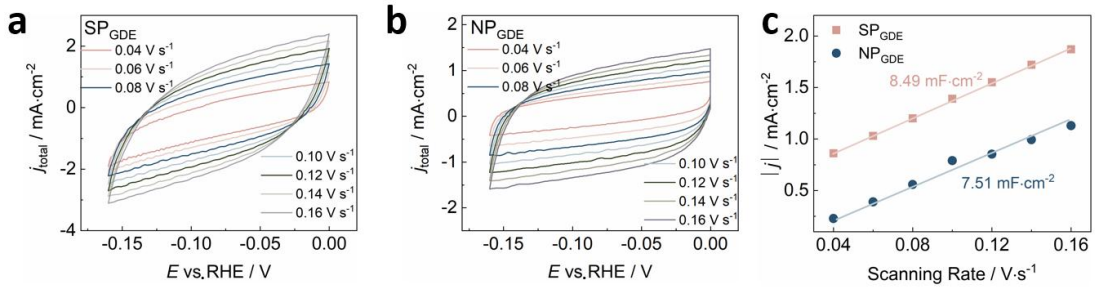

Fig. S17 Electrochemical double layer capacitance (EDLC) measurements.

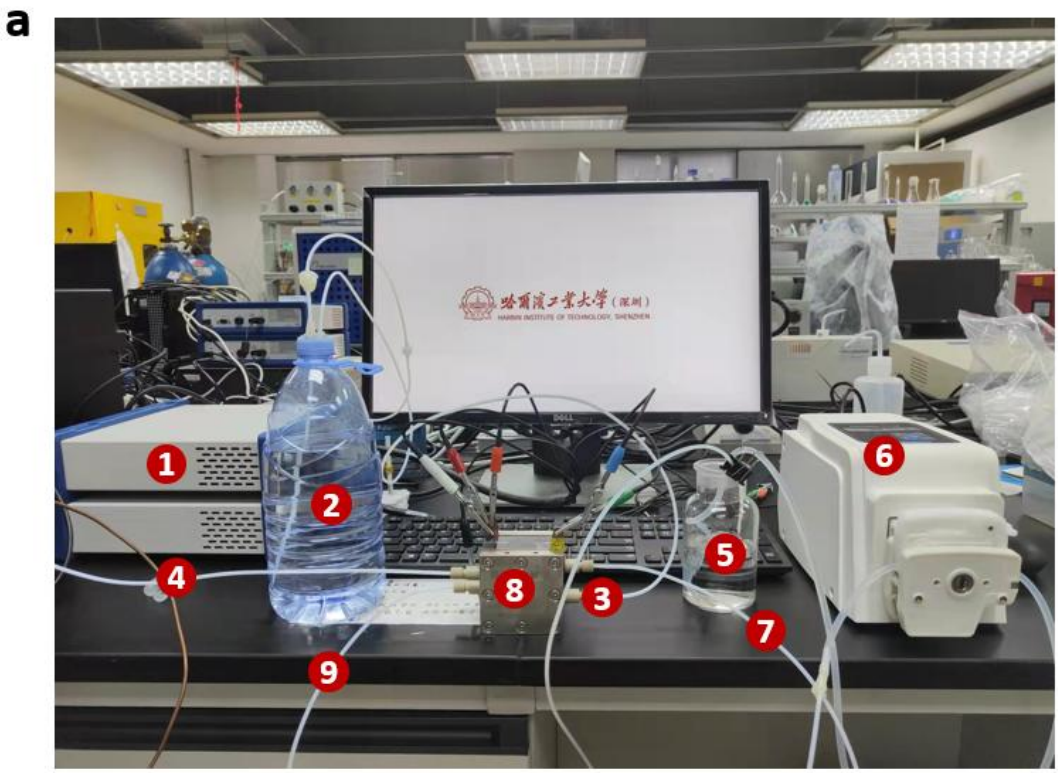

Fig. S18 A set of facility for conducting ECO_2RR in MEA. **(a)** The entire equipment, **(b)** Composition details of MEA.

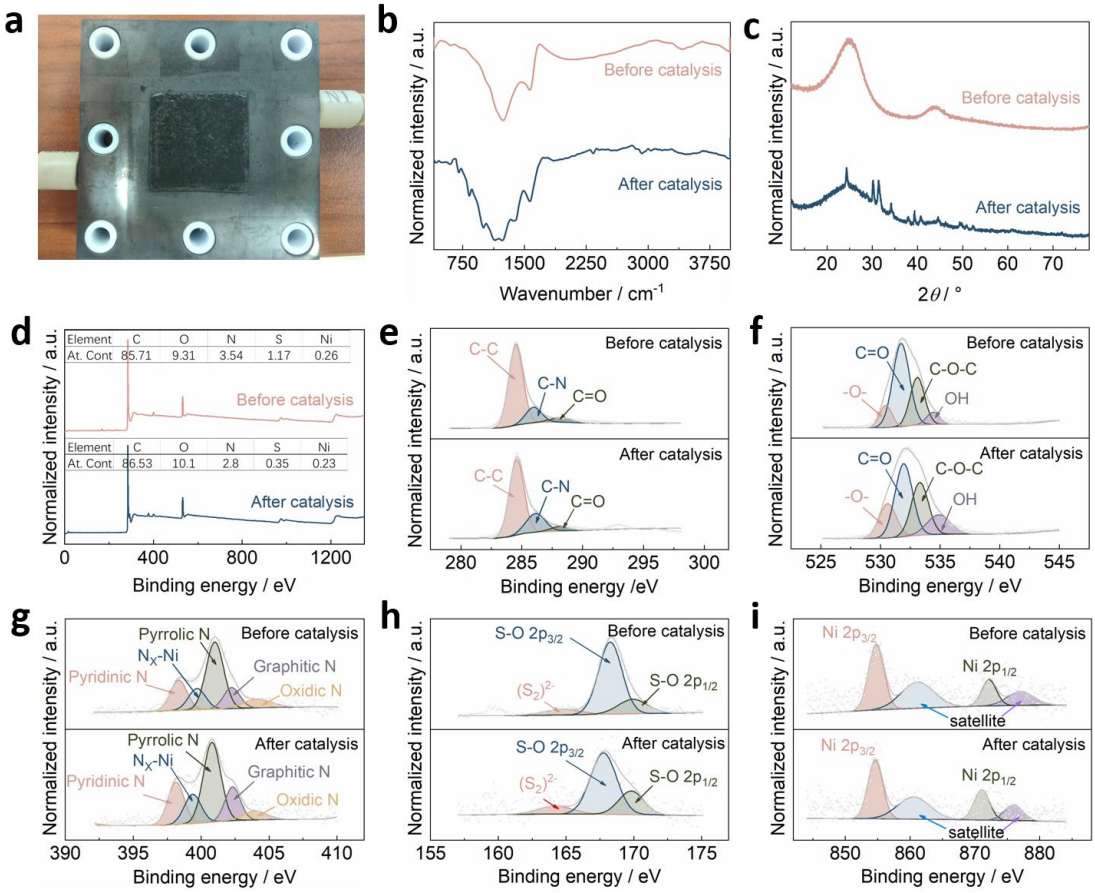

Fig. S19 SP_{GDE} properties comparison before and after electrolysis. **(a)** Photograph of SP_{GDE} after electrolysis. **(b)** FTIR spectra. **(c)** XRD spectra. **(d)** to **(i)** XPS spectra of overview, C 1s, O 1s, N 1s, S 2p and Ni 2p.

References

[1] K. Jiang, S. Siahrostami, T. Zheng, Y. Hu, S. Hwang, E. Stavitski, Y. Peng, J. Dynes, M. Gangisetty, D. Su, et al. 2018. Isolated Ni single atoms in graphene nanosheets for high-performance CO_2 reduction. Energy Environ. Sci. 11, 893–903.

[2] J. Chen, C. Li, G. Shi, 2013. Graphene materials for electrochemical capacitors. J. Phys. Chem. Lett. 4, 1244–1253.

[3] J. Gustavsson, C. Cederberg, U. Sonesson, R. Otterdijk, A. Meybeck, 2011. Global Food Losses and Food Waste- Extent, Causes and Prevention. Access at the website of www.fao.org

[4] Data reports. United States Department of Agriculture. Access at the website of pps.fas.usda.gov/psdonline/app

[5] World Food and Agriculture – Statistics Yearbook 2021. Food and Agriculture Organization of the United Nations.

[6] International news (2021). China Permeant Representation to UN Agencies for Food and Agriculture. Access at the website of www.cnafun.moa.gov.cn

[7] The State of Agriculture Markets 2020. (2021). Food and Agriculture Organization of the United Nations.

[8] OECD-FAO Agriculture Outlook 2019-2028. (2019). Organization for Economic Co-operation and Development, Food and Agriculture Organization of the United Nations.

[9] The State of World Fisheries and Aquaculture 2020. (2021). Food and Agriculture Organization of the United Nations.

[10] H. Yang, Q. Lin, C. Zhang, X. Yu, Z. Cheng, G. Li, Q. Hu, X. Ren, Q. Zhang, J. Liu, et al. 2020. Carbon dioxide electroreduction on single-atom nickel decorated carbon membranes with industry compatible current densities. Nat. Commun. 11, 1–8.